Seismic low-frequency anomalies in multiple reflections from thinly-layered poroelastic reservoirs

Beatriz Quintal and Stefan M. Schmalholz, Geological Institute, ETH Zurich*
Yuri Y. Podladchikov, PGP, University of Oslo
José M. Carcione, Instituto Nazionale di Oceanografia e di Geofisica Sperimentale (OGS)

Summary

Seismic low-frequency (1-10 Hz) anomalies in multiple reflections can be related to hydrocarbon-saturated rocks with high values of attenuation. We study reflections in the low-frequency range from a poroelastic layered reservoir embedded in an elastic background medium, using Biot's theory and 1D finite-difference modeling of wave propagation. In this model, the reservoir has a constant thickness and consists of a variable number of alternating pairs of fluid-saturated layers. For few layers (coarse layers), the reflections from the reservoir are identical when we compare results for poroelastic and equivalent elastic layers. For many layers (thin layers), the results are considerably different. When we choose, for example, the impedance of the background medium similar to the elastic Backus-averaged impedance of the reservoir, the reflections disappear in the elastic case, while in the poroelastic they become significant, due to velocity dispersion caused by wave-induced viscous fluid flow and attenuation between layers (interlayer-flow model).

Introduction

Recently, Korneev et al. (2004) showed that reflections from fluid-saturated layers have increased amplitude and delayed travel time when compared with reflections from gas-saturated layers. They consider laboratory and field measurements in the kHz and 1-20 Hz range, and explain the observed frequency-dependent reflections with very low values of the quality factor (< 5). They model low values of the quality factor by adding a diffusive term in the 1D elastodynamic wave equation, stating that the attenuation mechanism is still unclear. Their simple model predicts fairly well the low-frequency dependence of the difference between reflections from a reservoir measured in summer (gas filled) and winter (water filled).

High values of attenuation (i.e. low values of quality factor) in hydrocarbon-saturated layers have often been observed, and related reflections in the low-frequency range have recently attracted an increased interest in the scientific and industrial communities (e.g., Chapman et al., 2006; Goloshubin et al., 2006). Contrasts in attenuation at an interface increase the reflection amplitude (Bourbié et al., 1987, pp. 306). Low frequency spectral anomalies of the seismic wave field measured at the Earth surface may be generated by multiple reflections between the surface and hydrocarbon reservoirs. Spectral anomalies of microtremors in the 1-10 Hz range have been used as direct hydrocarbon indicator (Dangel et al., 2003; Graf et al., 2007). Here, we investigate spectral anomalies caused by multiple reflections from a reservoir with low values of the quality factor, using a physically-based model for low-frequency wave attenuation, referred to as one-dimensional (1D) interlayer-flow model (White et al., 1975; Norris, 1993, Gurevich and Lopatnikov, 1995; Müller and Gurevich, 2004; Carcione and Picotti, 2006; Carcione, 2007). This model is a 1D version of the so-called patchy-saturation models (e.g., White, 1975; Carcione et al., 2003; Pride et al., 2004; Toms et al., 2006). In these models, attenuation and velocity dispersion are caused by wave-induced viscous (dissipative) fluid flow, generated by fluid pressure differences in heterogeneous, saturated poroelastic materials. The wave propagation in such saturated poroelastic materials can be described mathematically with Biot's equations (Biot, 1962; Dutta and Odé, 1979). The interlayer-flow model, using realistic reservoir properties, is able to predict low values of the quality factor and significant velocity dispersion within the low 1-10 Hz frequency range (Carcione and Picotti, 2006). However, the unbounded analytical model, consisting of alternating pair of layers, cannot be used to evaluate the reflection coefficient of a finitely layered reservoir, and therefore we apply finite-difference simulations of wave propagation.

In our setup, the reservoir has constant thickness and is composed of a variable number of pairs of layers, i.e. variable layer thickness (Figure 1). One purpose is to evaluate the range of applicability of the analytical solution based on an infinite number of pairs of layers (White et al., 1975). Another objective is to model two physical transitions that are caused by varying the layer thickness; first, the transition from a heterogeneous coarsely-layered reservoir to an effective homogeneous reservoir (finely-layered, when Backus averaging applies), and second, the transition from the no-flow (high-frequency) to the quasi-static (low-frequency) limit.

Numerical method and experiments

We use the 1D elastodynamic equations and Biot's equations (Biot, 1962) to model wave propagation in elastic and poroelastic media, respectively, expressed as a first-

order velocity-stress formulation (Virieux, 1984). The four poroelastic equations are solved with an explicit finite-difference scheme using staggering in both space and time. For the poroelastic equations, we use a partition scheme (Carcione and Quiroga-Goode, 1995). The difference operators are second-order accurate in time and space. We successfully tested the numerical scheme versus analytical solutions of phase velocity and quality factor (White et al., 1975; Carcione and Picotti, 2006) (see Figure 4). The quality factor was calculated using the spectral-ratio and frequency-shift methods (Toksöz et al., 1979; Quan and Harris, 1997; Picotti and Carcione, 2006).

Figure 1 shows the model setup, in which source and receiver are at the same position, at the top. The source is a Gaussian pulse in time with maximum amplitude occurring at 0.1 s and characteristic e-fold decay frequency of 12 Hz. The receiver records the solid particle velocity during a total time of 2 s. A free surface is implemented at the top of the model and a non-reflecting boundary at the bottom. The reservoir is always 100 m thick and we vary only the number of layers so that the layer thickness decreases with increasing number of layers.

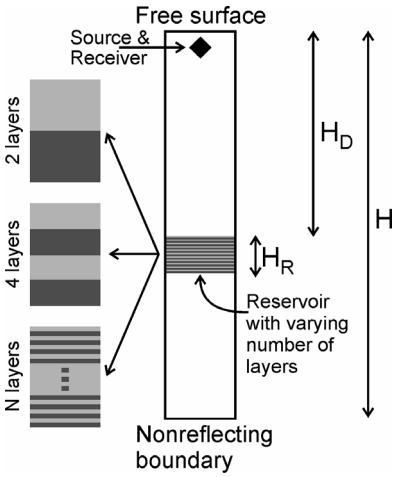

Figure 1. Model setup. The white part represents the background medium, grey is the water-saturated layer and black is the gas-saturated one. H_D = 300 m, H_R = 100 m and H = 400 m.

For our first experiment, the petrophysical properties are given in Table 1. Each pair of layers consists of one layer with slightly higher and one with slightly lower effective impedance than the background medium. In the poroelastic simulations the background medium is effectively elastic (porosity is set to 0.01). In the elastic simulations, we calculate the composite densities and equivalent P-wave velocities using low-frequency Gassmann's equations (< 10 Hz) (Gassmann, 1951; Bourbié et al., 1987; Carcione, 2007).

Table 1. Petrophysical parameters. K_b is the bulk modulus of the dry porous frame, K_s is the bulk modulus of the solid material , K_f is the bulk modulus of the pore fluid, ϕ is the porosity, ρ_s is the density of solid material, ρ_f is the density of pore fluid, μ is the shear modulus, k is the permeability, η is the viscosity, and V_P is the P-wave velocity in the saturated medium.

	Background medium	Water-saturated layer	Gas-saturated layer
K_b	6.6 GPa	6.6 GPa	6.6 GPa
K_s	8.588 GPa	28.9 GPa	28.9 GPa
K_f	2.3 GPa	2.3 GPa	0.022 GPa
ϕ	0.001	0.2	0.2
ρ_s	2360 kg/m^3	2700 kg/m^3	2700 kg/m^3
ρ_f	1000 kg/m^3	1000 kg/m^3	140 kg/m^3
μ	5.6 GPa	5.6 GPa	5.6 GPa
k	50 mD	50 mD	50 mD
η	1 Pa s	0.003 Pa s	10^{-5} Pa s
V_P	2607 m/s	2885 m/s	2541 m/s

We compute the Fourier spectra of the recorded particle velocity. The spectral anomalies are caused by constructive and destructive interferences of waves propagating between the reservoir and the free surface due to multiple reflections. Figure 2 shows the normalized spectra corresponding to 2, 32 and 500 layers. The normalization is done by dividing each spectrum by the spectrum of the particle velocity recorded in a simulation without reservoir (homogeneous background medium only). The spectra for the elastic and poroelastic cases are identical for 2 layers (Figure 2a), and increasing the number of layers, 32 layers (Figure 2b), causes a decrease of the amplitudes of spectral anomalies. Then, increasing the number of layers to 500 (Figure 2c) yields a spectrum for the poroelastic case remarkably different, compared to the elastic case. We define the peak strength (vertical lines plotted in Figure 2), which corresponds to the average vertical height of the spectral anomaly. Figure 3a shows peak strengths, at about 8 Hz, resulting from numerical simulations for 2, 8, 16, 32, 64, 128, 256, 500, 1000 and 2000 layers. In this experiment, the effective impedance of the finely-layered reservoir (6.11×10^6 kg/m^{2}s), calculated using the elastic Backus average (Backus, 1962; Mavko et al., 1998), is similar to the impedance of the background medium (6.15×10^6 kg/m^{2}s). Then, the peak strength in the elastic case decreases with increasing number of layers (i.e. decreasing layer thickness), and at around 32 layers, it

saturates at a very small value (due to low-impedance contrast). In the poroelastic case, the peak strength first decreases and, from around 32 layers, it increases with increasing number of layers, until saturating at about 2000 layers.

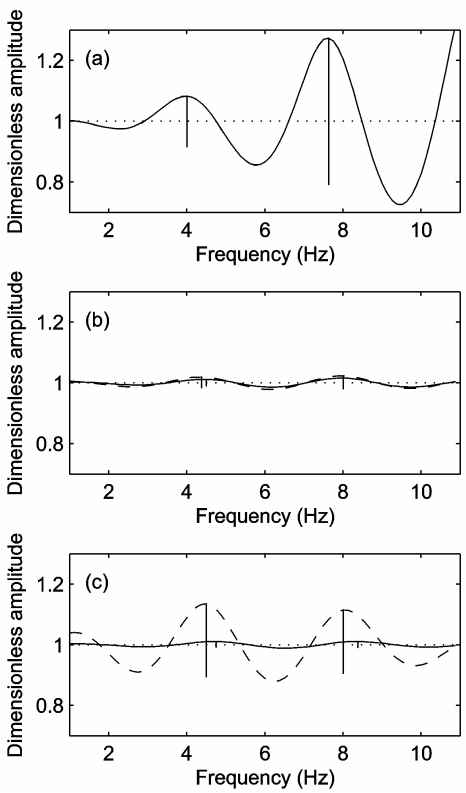

Figure 2. Normalized spectra of solid particle-velocity at the receiver position for 2 (a), 32 (b), and 500 layers (c). The dotted lines correspond to the spectra recorded in the absence reservoir (homogeneous background medium only). The solid and dashed curves correspond to the elastic and poroelastic spectra, respectively. In (a), elastic and poroelastic curves are identical and superposed. The vertical lines are the peak strengths at about 4 Hz and 8 Hz.

For the second experiment, we only changed properties of the background medium: the bulk modulus of dry matrix is changed to 6.1 GPa, and the bulk modulus of solid constituent is set to 6.25 GPa. The P-wave velocity calculated for this medium is 2411 m/s. In this case, the impedance of the background medium (5.69×10^6 kg/m^{2}s) is no more similar to the effective elastic Backus impedance of the finely-layered reservoir. Figure 3b shows that the peak strength in the elastic case saturates, as effective-medium theory applies, with a higher value (due to higher impedance contrast); however, in the poroelastic case, it decreases until saturating with a very small value.

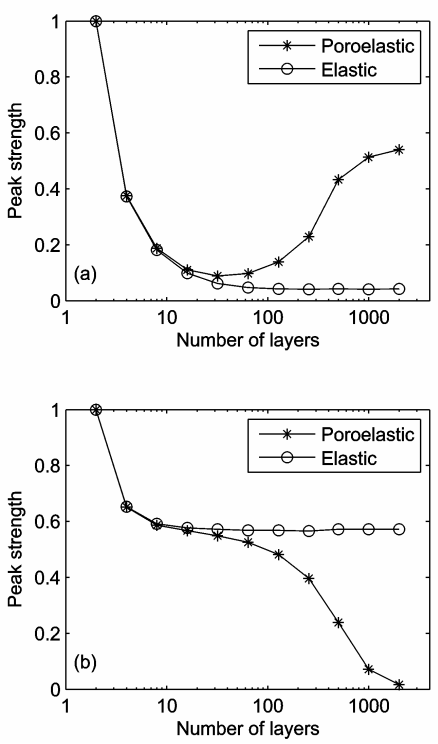

Figure 3. Variation of the peak strength with increasing number of layers (i.e. decreasing layer thickness). Peak strengths in (a) are calculated at about 8 Hz (Figure 2) and correspond to the case when the impedance of the background medium is similar to the effective elastic Backus impedance of the finely-layered reservoir. Peak strengths in (b) are calculated at about 6 Hz for a different background medium (different impedance).

Discussion

The results in Figures 2 and 3a imply that an elastic thinly-layered reservoir becomes "invisible" in the low-frequency range, when its effective elastic Backus impedance is similar to the impedance of the background medium. When the layers are poroelastic, the spectral anomalies first decrease like in the elastic case (while the reservoir is coarsely layered), and then increase with increasing number of layers. Increasing the number of layers causes a decrease of the layer thickness which shifts the velocity dispersion curve to higher frequencies (Figure 4a). As the layer thickness becomes smaller than the diffusion length scale of fluid flow, the behavior of the poroelastic rocks changes from the no-flow state (i.e. layer thickness much larger than diffusion length; high-frequency limit) to the quasi-static state (i.e. layer thickness much smaller than diffusion length; low-frequency limit). The diffusion length is given by $d = \sqrt{kN/\omega\eta}$, where ω is the angular frequency, $N = ML/H$, $M = \left[\phi/K_f + (\alpha-\phi)/K_s\right]^{-1}$, $\alpha = 1 - K_b/K_s$,

$L = K_b + 4\mu/3$, and $H = K_c + 4\mu/3$ (Gelinsky and Shapiro, 1997; Müller and Gurevich, 2004). The effective impedance of the layered medium, calculated with the poroelastic Backus average, in the quasi-static limit is 5.68×10^6 kg/m^{2}s, and in the no-flow limit it is 6.11×10^6 kg/m^{2}s (the last corresponds to the standard elastic Backus average, since it ignores fluid flow) (Gelinsky and Shapiro, 1997). Therefore, in the case of Figure 3a, the impedance contrast between the background medium (6.15×10^6 kg/m^{2}s) and the reservoir is about 0.6 % in the no-flow limit, while it is about 8 % in the quasi-static limit. In the case of Figure 3b, the background medium has impedance similar to the poroelastic Backus average in the quasi-static limit, then the impedance contrast between the background medium (5.69×10^6 kg/m^{2}s) and the reservoir is about 7 % in the no-flow limit and 0.2 % in the quasi-static limit.

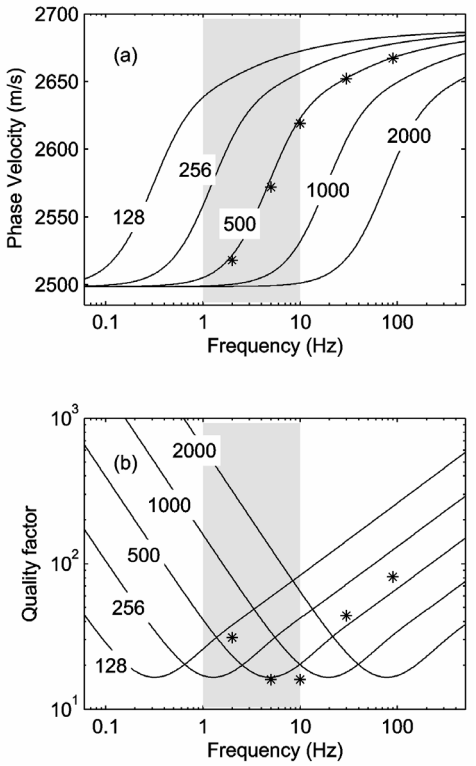

Figure 4. Analytical solution of White's 1D model (Carcione and Picotti, 2006), showing the phase velocity (a) and the quality factor (b) as a function of frequency, for different number of layers (or layer thicknesses). The star-symbols show results from finite-difference simulations for a layer thickness of 0.2 m (case of 500 layers), where the quality factor was calculated with the spectral ratio and frequency shift methods.

In the transition zone between no-flow and quasi-static limits, attenuation and velocity dispersion are significant. This is the case, for example, for 500 poroelastic layers (layer thickness of 0.2 m). For such medium, the diffusion length is 0.06 m for water-saturated layers and 0.13 m for gas-saturated layers, using the frequency of 5 Hz, at which the quality factor exhibits a minimum in the analytical solution of White's model (Figure 4).

In the applied setup the low- and high-frequency velocity limits, calculated using poroelastic Backus average, are identical to the ones calculated using Gassmann-Wood and Gassmann-Hill formulas (Toms et al., 2006; Mavko and Mukerji, 1998), respectively, because only the fluid type is changed from layer to layer (the latter account for partial saturation).

Conclusions

Wave-induced flow can cause significant attenuation and velocity dispersion in the low frequency range and within a narrow frequency band (1-10 Hz) for realistic petrophysical parameters (Figure 4). The change of the P-wave velocity from the high- to the low-frequency limit, caused by a change in layer thickness, significantly alters the reflectivity of a partially saturated layered reservoir. This effect does not appear in elastic models and, therefore, poroelastic models should be applied when studying reflections from hydrocarbon reservoirs in the low-frequency limit.

The numerical simulations show that the White analytical solution and the averaging theory for high- and low-frequency limits, valid for unbounded media, can be applied to reservoirs of finite thickness consisting only of a few hundred layers.

The interlayer-flow model discussed here provides a physical basis to the phenomenological attenuation model introduced by Korneev et al. (2004), and can explain the spectral anomalies observed at low frequencies in thinly-layered reservoirs.

Acknowledgements

This research has been supported by Spectraseis AG. B. Quintal and S. M. Schmalholz thank Tobias M. Müller for helpful discussions.

EDITED REFERENCES

Note: This reference list is a copy-edited version of the reference list submitted by the author. Reference lists for the 2007 SEG Technical Program Expanded Abstracts have been copy edited so that references provided with the online metadata for each paper will achieve a high degree of linking to cited sources that appear on the Web.

REFERENCES

Backus, G. E., 1962, Long-wave elastic anisotropy produced by horizontal layering: Journal of Geophysical Research, 67, 4427–4440.

Berryman, J. G., 1980, Long-wavelength propagation in composite elastic media, I. spherical inclusions: Journal of Acoustical Society of America, 68, 1809–1819.

Biot, M. A., 1962, Mechanics of deformation and acoustic propagation in porous media: Journal of Applied Physics, 33, 1482–1498.

Bourbié, T., O. Coussy, and B. Zinszner, 1987, Acoustics of porous media: E'ditions Technip.

Carcione, J. M., 2007, Wave fields in real media. Theory and numerical simulation of wave propagation in anisotropic, anelastic, porous and electromagnetic media: Handbook of Geophysical Exploration, 2nd ed., 38: Elsevier Science Publ. Co., Inc.

Carcione, J. M., H. B. Helle, and N. H. Pham, 2003, White's model for wave propagation in partially saturated rocks: Comparison with poroelastic numerical experiments: Geophysics, 68, 1389–1398.

Carcione, J. M., and S. Picotti, 2006, P-wave seismic attenuation by slow-wave diffusion: Effects of inhomogeneous rock properties: Geophysics, 71, no. 3, O1–O8.

Carcione, J. M., and G. Quiroga-Goode, 1995, Some aspects of the physics and numerical modeling of Biot compressional waves: Journal of Computational Acoustics, 3, 261–280.

Chapman, M., E. Liu, and X. Li, 2006, The influence of fluid-sensitive dispersion and attenuation on AVO analysis: Geophysical Journal International, 167, 89–105.

Dangel, S., M. E. Schaepman, E. P. Stoll, R. Carniel, O. Barzandji, E. D. Rode, and J. M. Singer, 2003, Phenomenology of tremor-like signals observed over hydrocarbon reservoirs: Journal of Volcanology and Geothermal Research, 128, 135–158.

Dutta, N. C., and H. Odé, 1979, Attenuation and dispersion of compressional waves in fluid filled porous rocks with partial gas saturation (White model) – Part I: Results: Geophysics, 44, 1777–1788.

Gassmann, F., 1951, Uber die elastizität porosër medien: Vierteljahrsschrift der Naturforschenden Gesellschaft in Zurich, 96, 1–23.

Gelinsky, S., and S. A. Shapiro, 1997, Poroelastic Backus averaging for anisotropic layered fluid- and gas-saturated sediments: Geophysics, 62, 1867–1878.

Goloshubin, G., C. Van Schuyver, V. Korneev, D. Silin, and V. Vingalov, 2006, Reservoir imaging using low frequencies of seismic reflections: The Leading Edge, 25, 527–531.

Graf, R., S. M. Schmalholz, Y. Podladchikov, and E. H. Saenger, 2006, Passive low frequency spectral analysis: Exploring a new field in geophysics: World Oil, 228, 47–52.

Gurevich, B., and S. L. Lopatnikov, 1995, Velocity and attenuation of elastic waves in finely layered porous rocks: Geophysical Journal International, 121, 933–947.

Korneev, V. A., G. M. Goloshubin, T. M. Daley, and D. B. Silin, 2006, Seismic low-frequency effects in monitoring fluid-saturated reservoirs: Geophysics, 69, 522–532.

Mavko, G., and T. Mukerji, 1998, Bounds on low frequency seismic velocities in partially saturated rocks: Geophysics, 63, 918-924.

Mavko, G., T. Mukerji, and J. Dvorkin, 1998, The rock physics handbook: Tools for seismic analysis in porous media: Cambridge University Press.

Müller, T.M., and B. Gurevich, 2004, One-dimensional random patchy saturation model for velocity and attenuation in porous rocks: Geophysics, 69, 1166–1172.

Norris, A. N., 1993, Low-frequency dispersion and attenuation in partially saturated rocks: Journal of the Acoustical Society of America, 94, 359–370.

Picotti, S., and J. M. Carcione, 2006, Estimating seismic attenuation (Q) in the presence of random noise: Journal of Seismic Exploration, 15, 165–181.

Pride, S. R., J. G. Berryman, and J. M. Harris, 2004, Seismic attenuation due to wave-induced flow: Journal of Geophysical Research, 109, B01201; http://dx.doi.org/10.1029/2003JB002639.

Quan, Y., and J. M. Harris, 1997, Seismic attenuation tomography using the frequency shift method: Geophysics, 62, 895–905.

Toksöz, M. N., D. H. Johnston, and A. Timur, 1979, Attenuation of seismic waves in dry and saturated rocks: I. Laboratory measurements: Geophysics, 44, 681–690.

Toms, J., T. M. Müller, R. Ciz, and B. Gurevich, 2006, Comparative review of theoretical models for elastic wave attenuation and dispersion in partially saturated rocks: Soil Dynamics and Earthquake Engineering, 26, 548–565.

Virieux, J., 1984, SH-wave propagation in heterogeneous media: Velocity-stress finite-difference method: Geophysics, 51, 889–901.

White, J. E., 1975, Computed seismic speeds and attenuation in rocks with partial gas saturation: Geophysics, 40, 224–232.
White, J. E., N. G. Mikhaylova, and F. M. Lyakhovitskiy, 1975, Low-frequency seismic waves in fluid saturated layered rocks: Izvestija Academy of Sciences USSR, Physics of the Solid Earth, 11, 654–659.